Journal of Nuclear Medicine, published on May 28, 2021 as doi:10.2967/jnumed.121.261906

Tumor sink effect in ^{68}Ga-PSMA-11 PET: Myth or Reality?

Andrei Gafita[1,2*], Hui Wang[2*], Andrew Robertson[2], Wesley R. Armstrong[1], Raphael Zaum[2], Manuel Weber[3], Farid Yagubbayli[2], Clemens Kratochwil[4], Tristan R. Grogan[5], Kathleen Nguyen[1], Fernando Navarro[2,6], Rouzbeh Esfandiari[7], Isabel Rauscher[2], Bjoern Menze[6,8], David Elashoff[5], Ebrahim S. Delpassand[7], Ken Herrmann[3], Johannes Czernin[1], Michael S. Hofman[9], Jeremie Calais[1], Wolfgang P. Fendler[3], Matthias Eiber[2]

[1]Ahmanson Translational Theranostics Division, Department of Molecular and Medical Pharmacology, University of California Los Angeles, Los Angeles, USA

[2]Department of Nuclear Medicine, Technical University Munich, Klinikum rechts der Isar, Munich, Germany

[3]Department of Nuclear Medicine, University of Duisburg-Essen and German Cancer Consortium (DKTK)-University Hospital Essen, Essen, Germany

[4]Department of Nuclear Medicine, Heidelberg University Hospital, Heidelberg, Germany

[5]Department of Medicine Statistics Core, David Geffen School of Medicine, University of California Los Angeles, Los Angeles, California.

[6]Department of Informatics, Technical University Munich, Munich, Germany

[7]Excel Diagnostics and Nuclear Oncology Center, Houston, USA

[8]Department of Quantitative Biomedicine, University of Zurich, Zurich, Switzerland

[9]Prostate Cancer Theranostics and Imaging Centre of Excellence (ProTIC), Molecular Imaging and Therapeutic Nuclear Medicine, Peter MacCallum Cancer Centre, Melbourne, VIC, Australia; Sir Peter MacCallum Department of Oncology, University of Melbourne, Melbourne, VIC, Australia

*authors contributed equally

Corresponding author: Andrei Gafita, MD

Ahmanson Translational Theranostics Division,

Department of Molecular and Medical Pharmacology,

David Geffen School of Medicine,

University of California, Los Angeles

200 Medical Plaza, Suite B114-61,

Los Angeles, CA 90095

Phone: +1 (310) 825-3617

E-mail: agafita@mednet.ucla.edu

Abstract: 306 words

Manuscript: 3774 words

Running Title: Tumor sink effect in PSMA PET

Financial Support: This work was partially supported by the Jonsson Comprehensive Cancer Center fellowship award.

ABSTRACT

Background: We aimed to systematically determine the impact of tumor burden on the ^{68}Ga-prostate-specific membrane antigen-11 (^{68}Ga-PSMA) PET biodistribution by the use of quantitative measurements.

Methods: This international multicenter retrospective analysis included 406 men with prostate cancer who received ^{68}Ga-PSMA PET/CT. Of these, 356 had positive findings and were stratified by quintiles into very low (Q1, ≤25 ml), low (Q2, 25-189 ml), moderate (Q3, 189-532 ml), high (Q4, 532-1355 ml) and very high (Q5, ≥1355 ml) total PSMA-positive tumor volume (PSMA-VOL). PSMA-VOL was obtained by semi-automatic segmentation of total tumor lesions using qPSMA software. Fifty prostate cancer patients with no PSMA-positive lesions (negative scan) served as control group. Normal organs, which included salivary glands, liver, spleen and kidneys, were semi-automatically segmented using ^{68}Ga-PSMA PET images and average SUV (SUV_{mean}) was obtained. Correlations of PSMA-VOL as continuous and as categorical variable by quintiles with SUV_{mean} of normal organ were evaluated.

Results: The median PSMA-VOL was 302 ml (interquartile range [IQR], 47-1076). The median (IQR) SUV_{mean} of salivary glands, kidneys, liver and spleen was 10.0 (7.7-11.8), 26.0 (20.0-33.4), 3.7 (3.0-4.7) and 5.3 (4.0-7.2), respectively. PSMA-VOL showed a moderate negative correlation with SUV_{mean} of salivary glands (r=-0.44, p<0.001), kidneys (r=-0.34, p<0.001), and liver (r=-0.30, p<0.001) and a weak negative correlation with spleen SUV_{mean} (r=-0.16, p=0.002). Patients with very high PSMA-VOL (Q5, ≥1355 ml) had a significant lower PSMA uptake of salivary glands, kidneys, liver and spleen

compared to the control group with an average difference of -38.1%, -40.0%, -43.2% and -34.9%, respectively (p<0.001).

Conclusion: Tumor sequestration affects ^{68}Ga-PSMA biodistribution in normal organs. Patients with very high tumor load showed a significant lower uptake of ^{68}Ga-PSMA in normal organs confirming a tumor sink effect. As similar effects might occur with PSMA-targeted radioligand therapy, these patients might benefit from increased therapeutic activity without exceeding the radiation dose limit for organs at risk.

Key Words: PET; tumor sink effect; prostate cancer; PSMA; Ga-PSMA; radioligand therapy

INTRODUCTION

The biodistribution of radiolabeled prostate-specific membrane antigen (PSMA)-ligands in prostate cancer patients reflects a complex interaction between tracer uptake, retention and excretion in pathological and normal tissues. Accumulation of PSMA-ligands is also observed in non-tumoral tissues, such as liver, spleen, kidneys and salivary glands, which have shown to exhibit a high variability in tracer uptake (*1*). In clinical practice, it is observed that the relative accumulation of PSMA-ligands in normal tissue is inversely related to the PSMA-positive tumor burden. This phenomenon is commonly referred to as *tumor sink effect* in which high tracer uptake in extensive tumor masses reduces tracer accumulation in normal tissues (*2-4*).

PSMA-targeted radioligand therapy with Lutetium-177 (^{177}Lu-PSMA-RLT) demonstrated positive results in phase II trials of men with metastatic castration-resistant prostate cancer (mCRPC) (*5-7*) and is currently investigated in metastatic hormone-sensitive prostate cancer setting (*8*). If confirmed, a tumor sink effect might have implications for ^{177}Lu-PSMA-RLT by providing the rationale for individual adaptation of therapeutic dosages to the patient tumor load (*9*). Patients with high tumor load might benefit from higher injected activity per cycle without exceeding radiation dose limit in organs at risk, particularly the salivary glands and the kidneys which are considered dose limiting organs (*10*).

Besides their therapeutic use, PSMA-ligands have also been used for diagnostic purposes using tumor-specific whole-body PET imaging (e.g. ^{68}Ga-PSMA-11 [^{68}Ga-PSMA])(*11*). ^{68}Ga-PSMA PET imaging provides reliable estimates of the biodistribution

of therapeutic PSMA ligands (*12*). Several reports have previously investigated the sink effect in PSMA-targeted PET, however, the data reported are contradictory (*13,14*).

To address this question, we aimed here to quantify the effect of tumor burden on ^{68}Ga-PSMA PET organ biodistribution by the use of quantitative measurements. We hypothesized that the tumor sequestration of the injected radiopharmaceutical in patients with high disease burden leads to a significant decrease of uptake in non-tumoral tissue.

METHODS

Study Design and Patient Population

Data of men with histologically proven prostate cancer who underwent ^{68}Ga-PSMA PET imaging at six institutions were screened retrospectively. This international multicenter study was designed to include patients with both PSMA-positive and PSMA-negative PET scans. First, two pre-established databases of patients with known metastatic disease on ^{68}Ga-PSMA PET were screened: i) a dataset of men with metastatic hormone-sensitive prostate cancer who received ^{68}Ga-PSMA PET in the setting of initial staging or biochemical recurrence (n=100) and ii) a dataset of men with mCRPC who received ^{68}Ga-PSMA PET before initiation of ^{177}Lu-PSMA-RLT (*15,16*) (n=285). Second, 50 men with biochemical recurrence after definitive treatment of prostate cancer who had no tumor lesions on ^{68}Ga-PSMA PET were randomly selected from institution database (*17*) to serve as control group. The flowchart of this study is displayed in Figure 1. Inclusion criteria were imaging with ^{68}Ga-PSMA11 PET/CT and data evaluable by the segmentation

software. Patients who received an ^{18}F-labelled PSMA PET/CT or PSMA-targeted PET/MR imaging were excluded.

Of 435 screened men with prostate cancer, 406 were eligible and included. Overall, 162 (40%) patients received the scan in a prospective setting (NCT02940262, NCT03042312, ACTRN12615000912583), while 244 (60%) received the scan under compassionate access programs. In a subanalysis, we identified 20 patients from the mCRPC cohort who had high disease burden on the baseline ^{68}Ga-PSMA PET at the initiation of ^{177}Lu-PSMA-RLT and received a follow-up scan after two treatment cycles, as described (*18*) (Fig. 1). All scans were performed between October 2014 and August 2019. All patients gave written consent to undergo clinical ^{68}Ga-PSMA PET scan. Necessity for study specific consent was waived by the Ethics Committee.

Outcomes

The primary objective of this study was to determine the impact of total tumor burden on ^{68}Ga-PSMA uptake in normal organs on PET imaging. Based on reproducibility data which showed a normal variability up to 30% between two SUV measurements of normal organs (*19,20*), the tumor sink effect was a priori defined as a 30% or greater decline in ^{68}Ga-PSMA uptake in normal organs compared to the control group.

The secondary objective was to determine the impact of changes in tumor volume on ^{68}Ga-PSMA normal organ uptake and appearance of new lesions on the interim PET scan after two cycles of ^{177}Lu-PSMA-RLT. Patients were stratified into responders versus non-responders to ^{177}Lu-PSMA-RLT based on the PSMA tumor volume decline of 30% on the interim PET scan, as described (*18*).

Imaging Protocol

Patients received an average±SD of 155±53 MBq ^{68}Ga-PSMA-HBED-CC (PSMA-11) via complete intravenous injection. Image acquisition was started after an average±SD of 64±17 minutes post-injection. Static, whole-body images were used (mid thighs to skull vertex). All scans were corrected for decay, scatter, and random coincidences. Photon attenuation was performed using CT. Images were acquired using GE Discovery 710 (n=50), Siemens Biograph mCT (n=244), Siemens Biograph 64 (n=92) and Siemens Biograph 16 (n=20) scanners. All images were obtained in accordance with the ^{68}Ga-PSMA11 PET joint EANM/SNMMI guideline, ensuring harmonized quantification (*21*). Standard, vendor-provided image reconstructions were used. The applied reconstruction parameters are summarized in Supplementary Table 1.

Image Analyses

Tumor segmentation was performed centrally by a nuclear medicine physician using qPSMA software (*22*) to obtain total PSMA-positive tumor volume (PSMA-VOL). PSMA-VOL was categorized into five groups based on quintiles: very low (Q1: ≤20th percentile), low (Q2: 20th-40th percentile), moderate (Q3: 40th-60th percentile), high (Q4: 60th-80th percentile), and very high (Q5: ≥80th percentile). Organs which typically exhibit moderate to high PSMA-ligand uptake were assessed: salivary glands, kidneys, liver and spleen (*23*). The entire volume of each normal organ was segmented automatically using an in-house algorithm. The annotations obtained using the automatic algorithm were reviewed by a nuclear medicine physician using PET images and adjusted manually when

necessary. The average and maximum standardized uptake value (SUV_{mean} and SUV_{max}) not corrected for lean body mass or body surface area were obtained to measure ^{68}Ga-PSMA uptake in normal organs. Analysis of the liver was not performed in patients with PSMA-positive liver metastases. Salivary glands not entirely included in the PET field-of-view were excluded from the analysis.

Statistical Analyses

Values were reported as mean ± standard deviation or median (interquartile range [IQR]). Correlations between PSMA-VOL and normal organ tracer uptake were evaluated using the Spearman's correlation coefficient rho with a two-tailed test for significance. Kruskal-Wallis test was performed to compare the degree of ^{68}Ga-PSMA uptake in normal organs among the six tumor burden groups (control, very low, low, moderate, high, and very high). The differences among groups were tested for significance against no-difference. A *P* value ≤ 0.05 was considered statistically significant. The *P* values were not adjusted for multiple testing. Analyses were performed using SPSS Statistics v26.0 (IBM Corp., USA) and R Statistics (version 3.4.0).

RESULTS

Population characteristics are summarized in Table 1. Analysis of liver uptake was not performed in 40 patients due to PSMA-positive liver metastases. Salivary glands of two patients could not be delineated and were excluded from the analysis.

Tumor Volume and Organ SUV Measurements

The median SUV_{mean} of salivary glands, kidneys, liver, and spleen was 10.0 (IQR, 7.7-11.8), 26.0 (IQR, 20.0-33.4), 3.7 (IQR, 3.0-4.7) and 5.3 (IQR, 4.0-7.2), respectively (Fig. 2), while the median SUV_{max} was 21.3 (IQR, 16.9-27.0), 51.8 (IQR, 37.8-67.9), 9.7 (IQR, 7.8-11.8) and 10.1 (IQR, 8.0-12.8) (Supplementary Fig. 1). The median PSMA-VOL was 302 ml (IQR, 47-1076). The 20^{th}, 40^{th}, 60^{th}, 80^{th} percentile of PSMA-VOL was 25 ml, 189 ml, 532 ml, and 1355 ml, respectively. The median PSMA-VOL in the very low (n=71), low (n=71), moderate (n=71), high (n=72), and very high (n=71) group was 5 ml (IQR, 2-11), 76 ml (IQR, 46-123), 302 ml (IQR, 235-387), 899 ml (IQR, 685-1078), and 2336 ml (IQR, 1852-3080), respectively. Examples of ^{68}Ga-PSMA PET studies for each tumor volume group are presented in Figure 3.

Correlations of Tumor Volume with Normal Organ Uptake

PSMA-VOL showed a statistically significant moderate negative correlation with SUV_{mean} of salivary glands (r=-0.44, p<0.001), kidneys (r=-0.34, p<0.001), and liver (r=-0.30, p<0.001) and a statistically significant weak negative correlation with spleen SUV_{mean} (r=-0.16, p=0.002). PSMA-VOL showed a statistically significant moderate negative correlation with SUV_{max} of salivary glands (r=-0.35, p<0.001) and a statistically significant weak negative correlation with kidneys (r=-0.26, p<0.001), liver (r=-0.23, p<0.001), and spleen SUV_{max} (r=-0.19, p<0.001).

Normal Organ Uptake Stratified by Tumor Volume Groups

The absolute values and differences in SUVs of normal organs in the very low, low, moderate, high, and very high PSMA-VOL compared to the control group are given in Table 2 and displayed in Figure 4 and Supplementary Figure 2. In general, higher PSMA-VOL was associated with lower ^{68}Ga-PSMA uptake in normal organs.

The SUV_{mean} of salivary glands, kidneys, liver and spleen was significantly lower in patients with very high PSMA-VOL compared to the control group (p<0.001) with an average (95%CI) difference of -38.1 (-47.8, -29.7) %, -40.0 (-50.3, -31.1) %, -43.2 (-55.6, -30.8) %, and -34.9 (-49.8, -21.3) %, respectively.

The SUV_{max} of salivary glands, kidneys and liver was significantly lower in patients with very high PSMA-VOL compared to the control group (p<0.05) with an average (95%CI) difference of -26.6 (-38.9, -15.1) %, -28.4 (-39.4, -18.0) %, and -17.9 (-30.0, -4.2) %, respectively.

Changes in Tumor Volume and Normal Uptake

Of 20 patients included in this analysis, 10 (50%) were responders achieving a PSMA-VOL decline ≥30% on the interim scan relative to baseline. The average (95%CI) change in PSMA-VOL in responders was -47.0 (-55.7, -38.4) %, while in non-responders was +6.3 (-14.4, +26.9) %. The average (95%CI) difference in SUV_{mean} of salivary glands, liver, kidneys and spleen in responders was +61.1 (-3.5, +125.7; p=0.06) %, +33.4 (-17.2, +83.9; p=0.17) %, +74.0 (+8.7, +139.2; p=0.03) %, and +61.8 (+21.4, +102.2; p=0.007) %, respectively. In non-responders, the average (95%CI) change in salivary glands, kidneys, liver and spleen was -2.5 (-15.3, +10.3; p=0.67) %, +10.7 (-6.1, +28.3; p=0.07) %, +12.1 (-6.1, +30.3; p=0.16) %, and +23.8 (-18.9, +66.5; p=0.24) %, respectively.

Individual changes of PSMA-VOL, SUV_{mean} and SUV_{max} for normal organs in ^{68}Ga-PSMA PET are given in Supplementary Table 2. Appearance of new PSMA-positive lesions on interim scan was observed in one (10%) responder and seven (70%) non-responder patients.

DISCUSSION

In this multicenter retrospective analysis, patients with high tumor burden demonstrated significantly lower normal organ uptake on ^{68}Ga-PSMA PET. Our primary endpoint of a SUV difference numerically greater than 30% in salivary glands and kidneys compared to the control group was met in patients with very high tumor volume (≥1355 ml).

Controversial results on the tumor sink effect in PSMA-targeted PET have been reported. Gaertner et al. (*13*) found a decline of 36-43%, 45%, 25% and 19% of ^{68}Ga-PSMA uptake in salivary glands, kidneys, liver and spleen, respectively, in mCRPC patients who were classified visually as having PSMA-positive PET high tumor burden. In contrast, Werner et al. (*14*) found in ^{18}F-DCFPyL PET a significant correlation only for kidneys uptake with PSMA-VOL. However, these results are not surprising, since only patients with early-stage prostate cancer having low tumor burden were included (median PSA: 3.2 ng/ml) whereas a sink effect is expected to occur at high tumor volume levels. Limitations of these studies also include small sample size, which was not powered for uptake correlation, use of a small regions-of-interest for measuring tracer uptake in large organs (e.g. liver or spleen) and visual assessment of disease burden. To overcome these, in the present analysis we segmented semi-automatically on ^{68}Ga-PSMA PET the total disease burden and the entire volume of normal organs. Moreover, for a complete understanding of the associations between disease burden and normal uptake, we

included patients from the entire spectrum of prostate cancer and categorized them into six subgroups: PSMA-negative, very low, low, moderate, high and very high tumor volume.

The highest correlation of normal organ uptake with tumor burden was noticed in salivary glands, followed by kidneys, liver and, at a lower degree, by spleen. However, SUV_{mean} of kidneys and liver was significantly lower beginning with patients with low tumor volume (25-189 ml), whereas for salivary glands only in patients with high (532-1355 ml) and very high tumor volume (≥1355 ml). As compared to SUV_{mean}, we observed weaker correlations for SUV_{max} of normal organs with tumor burden. This observation underlines the importance of using SUV_{mean} over SUV_{max} for measuring tracer uptake in normal organs in PET imaging, which captures the entire organ uptake and does not limit to one voxel. Two limitations of SUV_{max} are worth mentioning here: the variability when structures with heterogeneous uptake are measured (e.g. liver) and the dependence on the reconstruction parameters (e.g. potential use of point-spread-function). This can have important implication, particularly in a multicentric setting where the harmonization protocol can affect SUV_{max} findings.

Our study has clinical implications. When performing PSMA-targeted RLT, the therapeutic activity is limited because of potential toxicity to organs at risk. Salivary glands and kidneys are the main critical organs with highest absorbed dose (*10*). Moreover, xerostomia was reported as the main reason for treatment discontinuation during ^{225}Ac-PSMA-RLT (*24*). Our findings suggest that candidates for ^{177}Lu-PSMA-RLT with a very high tumor volume (≥1355 ml for our analysis defined by quintiles) on the screening

PSMA-PET have a significantly lower normal organ uptake and might benefit from an increased therapeutic activity without exceeding the radiation dose limit for organs at risk.

A first attempt towards individualizing therapeutic activity for ^{177}Lu-PSMA-RLT was made by Hofman et al. (*5*), where ^{177}Lu-PSMA-617 activity was increased up to 20% in heavily metastasized patients. Dosimetry data from the same cohort showed that higher absorbed dose to tumor was associated with higher rates of PSA response and that tumor volume delineated on pre-therapeutic ^{68}Ga-PSMA PET is inversely correlated with salivary glands and kidneys absorbed radiation dose (*25*). Hence, the sink effect may represent a great opportunity for ^{177}Lu-PSMA-RLT to safely increase therapeutic activity to achieving an improved antitumor efficacy. Besides toxicity, it might be also logical to administer a higher amount of treatment activity when the tumor load is higher, in order to avoid undertreatment.

Overall, the present study establishes tumor sequestration as a major factor affecting ^{68}Ga-PSMA biodistribution in patients with high disease burden, which leads to a sink effect that decreases activity concentration in normal organs. In addition, we found that changes in tumor volume during ^{177}Lu-PSMA-RLT impact the normal uptake on the follow-up ^{68}Ga-PSMA PET images. This emphasizes the potential utility of repeated dosimetry studies during ^{177}Lu-PSMA-RLT when individualizing therapeutic dosage. Only one patient (without a decrease in ^{68}Ga-PSMA uptake of normal organs; Supplementary Table 2) had appearance of new lesions on the follow-up scan, suggesting that appearance of new lesions on PSMA post-treatment scans are likely to be treatment-related. Nevertheless, additional studies investigating the impact of sink effect on intra-tumor heterogeneity are warranted to provide additional insights on this phenomenon.

Strengths of this study include the multicenter setting, large patient population, the use of full quantitative measurements for tumor burden assessment. The major limitation of this study is the use of single static PET image protocol and thus, our results should be interpreted with caution in the framework of ^{177}Lu-PSMA-RLT. In addition, we are unable to analyze the influence of potential effects arising from different specific activities. However, given the low half-life of ^{68}Ga and a standardized production no large scale (>10^2) difference might be present. Further, we used only SUV normalized to body weight as a quantitative parameter of PET signal. Alternative quantitative parameters have been described in the literature, i.e. SUV normalized to lean body mass (SUL)(*26*) or uptake ratio to blood-pool (*27*), however, only at a research level. Further studies to supporting their implementation in clinical practice are awaited. Correlations with dosimetry data with multiple time points are warranted to establish pre-therapeutic PSMA-targeted PET as a quantitative tool for individualizing therapeutic doses.

CONCLUSION

Tumor sequestration affects ^{68}Ga-PSMA biodistribution by decreasing activity concentration in normal organs confirming the tumor sink effect. A relevant sink effect was noticed in patients with very high tumor burden (≥1355 ml). Due to favorable uptake ratios, PSMA-targeted RLT with increased activity regimens should be assessed in patients with very high tumor volume. Repeated dosimetry during PSMA-targeted RLT should be considered to not miss the impact of changes in tumor burden on dose distribution. Further studies are warranted to establishing pre-therapeutic PSMA-targeted PET as a tool for individual activity adaptation of PSMA-targeted RLT.

FINANCIAL SUPPORT

AG is the recipient of the Jonsson Comprehensive Cancer Center fellowship award and Dr. Christiaan Schiepers postdoctoral fellowship award. JCa is supported by the Prostate Cancer Foundation (2020 Young Investigator Award 20YOUN05, 2019 Challenge Award 19CHAL02) and the Society of Nuclear Medicine and Molecular Imaging (2019 Molecular Imaging Research Grant for Junior Academic Faculty). MSH is supported by grants from the Prostate Cancer Foundation (PCF), Movember Foundation, Australian Government Medical Research Future Fund (MRFF), Prostate Cancer Foundation of Australia (PFCA) and U.S. Department of Defence. WPF received financial support from the German Research Foundation (Deutsche Forschungsgemeinschaft, DFG, grant FE1573/3-1 / 659216), Mercator Research Center Ruhr (MERCUR, An-2019-0001), IFORES (D/107-81260, D/107-30240), Doktor Robert Pfleger-Stiftung, and Wiedenfeld-Stiftung/Stiftung Krebsforschung Duisburg. HW received financial support from the China Scholarship Council (CSC). FN received financial support from the German Research Foundation (Deutsche Forschungsgemeinschaft, DFG, research training group grant GRK 2274).

CONFLICT OF INTEREST

JCa reports prior consulting activities outside of the submitted work for Advanced Accelerator Applications, Blue Earth Diagnostics, Curium Pharma, GE Healthcare, Janssen Pharmaceuticals, Progenics Pharmaceuticals, Radiomedix and Telix Pharmaceuticals. ME reports prior consulting activities for Blue Earth Diagnostics, Progenics Pharmaceuticals and Point Biopharma and a patent application for rhPSMA outside of the submitted work. JCz is a founder, board member, and holds equity in Sofie

biosciences and Trethera Therapeutics. Intellectual property is patented by the University of California and licensed to Sofie Biosciences and Trethera Therapeutics. JCz was a consultant for Endocyte Inc. (VISION trial steering committee), Actinium Pharmaceuticals and Point Biopharma outside of the submitted work. MSH reports honoraria for lectures from Astellas, Janssen, Mundipharma; advisory fees from Merck/MSD. No other potential conflict of interest relevant to this article was reported. KH reports personal fees from Bayer, personal fees and other from Sofie Biosciences, personal fees from SIRTEX, non-financial support from ABX, personal fees from Adacap, personal fees from Curium, personal fees from Endocyte, grants and personal fees from BTG, personal fees from IPSEN, personal fees from Siemens Healthineers, personal fees from GE Healthcare, personal fees from Amgen, personal fees from Novartis, personal fees from ymabs, personal fees from Bain Capital, personal fees from MPM Capital outside the submitted work. WPF was a consultant for Endocyte and BTG, and he received fees from RadioMedix and Bayer outside of the submitted work. No other potential conflict of interest relevant to this article was reported.

KEY POINTS

QUESTION: Does the tumor burden impact the biodistribution of ^{68}Ga-PSMA-11 PET?

PERTINENT FINDINGS: In this international multicenter retrospective study, we observed a significant negative correlation between PSMA-positive tumor burden and ^{68}Ga-PSMA-11 PET uptake in normal organs, i.e. salivary glands, kidneys, liver and spleen. Patients with very high tumor burden (≥1355 ml for our analysis defined by quintiles) had a significantly lower uptake of ^{68}Ga-PSMA-11 in normal organs.

IMPLICATIONS FOR PATIENT CARE: Our findings suggest that candidates for PSMA-targeted radioligand therapy with a very high tumor volume on the screening PSMA-PET have significantly lower normal organ uptake and might benefit from an increased therapeutic activity without exceeding the radiation dose limit for organs at risk.

GRAPHICAL ABSTRACT

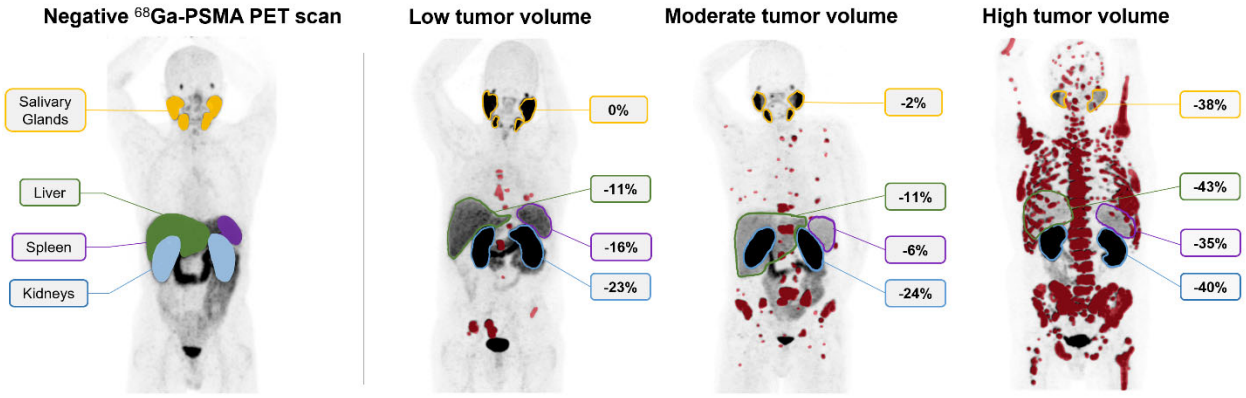

REFERENCES

1. Pfob CH, Ziegler S, Graner FP, et al. Biodistribution and radiation dosimetry of (68)Ga-PSMA HBED CC-a PSMA specific probe for PET imaging of prostate cancer. *Eur J Nucl Med Mol Imaging.* 2016;43:1962-1970.

2. Beauregard JM, Hofman MS, Kong G, Hicks RJ. The tumour sink effect on the biodistribution of 68Ga-DOTA-octreotate: implications for peptide receptor radionuclide therapy. *Eur J Nucl Med Mol Imaging.* 2012;39:50-56.

3. Viglianti BL, Wale DJ, Wong KK, et al. Effects of tumor burden on reference tissue standardized uptake for PET imaging: Modification of PERCIST Criteria. *Radiology.* 2018;287:993-1002.

4. Love C, Din AS, Tomas MB, Kalapparambath TP, Palestro CJ. Radionuclide bone imaging: an illustrative review. *Radiographics.* 2003;23:341-358.

5. Hofman MS, Violet J, Hicks RJ, et al. [(177)Lu]-PSMA-617 radionuclide treatment in patients with metastatic castration-resistant prostate cancer (LuPSMA trial): a single-centre, single-arm, phase 2 study. *Lancet Oncol.* 2018;19:825-833.

6. Emmett L, Crumbaker M, Ho B, et al. Results of a prospective phase 2 pilot trial of (177)Lu-PSMA-617 therapy for metastatic castration-resistant prostate cancerincluding imaging predictors oftreatment response and patterns of progression. *Clin Genitourin Cancer.* 2019;17:15-22.

7. Violet J, Sandhu S, Iravani A, et al. Long-term follow-up and outcomes of retreatment in an expanded 50-patient single-center phase II prospective trial of (177)Lu-PSMA-617 theranostics in metastatic castration-resistant prostate cancer. *J Nucl Med.* 2020;61:857-865.

8. Privé BM, Janssen MJR, van Oort IM, et al. Lutetium-177-PSMA-I&T as metastases directed therapy in oligometastatic hormone sensitive prostate cancer, a randomized controlled trial. *BMC Cancer.* 2020;20:884.

9. Hofman MS, Hicks RJ. Peptide receptor radionuclide therapy for neuroendocrine tumours: standardized and randomized, or personalized? *Eur J Nucl Med Mol Imaging.* 2014;41:211-213.

10. Okamoto S, Thieme A, Allmann J, et al. Radiation dosimetry for (177)Lu-PSMA I&T in metastatic castration-resistant prostate cancer: absorbed dose in normal organs and tumor lesions. *J Nucl Med.* 2017;58:445-450.

11. Hofman MS, Lawrentschuk N, Francis RJ, et al. Prostate-specific membrane antigen PET-CT in patients with high-risk prostate cancer before curative-intent surgery or radiotherapy (proPSMA): a prospective, randomised, multicentre study. *Lancet.* 2020;395:1208-1216.

12. Wang J, Zang J, Wang H, et al. Pretherapeutic 68Ga-PSMA-617 PET may indicate the dosimetry of 177Lu-PSMA-617 and 177Lu-EB-PSMA-617 in main organs and tumor lesions. *Clin Nucl Med.* 2019;44:431-438.

13. Gaertner FC, Halabi K, Ahmadzadehfar H, et al. Uptake of PSMA-ligands in normal tissues is dependent on tumor load in patients with prostate cancer. *Oncotarget.* 2017;8:55094-55103.

14. Werner RA, Bundschuh RA, Bundschuh L, et al. Semiquantitative parameters in PSMA-Targeted PET imaging with [(18)F]DCFPyL: impact of tumor burden on normal organ uptake. *Mol Imaging Biol.* 2020;22:190-197.

15. Gafita A, Fendler WP, Hui W, et al. Efficacy and Safety of (177)Lu-labeled prostate-specific membrane antigen radionuclide treatment in patients with diffuse bone marrow involvement: a multicenter retrospective study. *Eur Urol.* 2020;78:148-154.

16. Gafita A, Calais J, Wang H, et al. Prognostic markers for overall survival and outcome to LuPSMA radionuclide treatment in patients with metastatic castration-resistant prostate cancer. *J Clin Oncol.* 2020;38:5548-5548.

17. Fendler WP, Calais J, Eiber M, et al. Assessment of 68Ga-PSMA-11 PET accuracy in localizing recurrent prostate cancer: a prospective single-arm clinical trial. *JAMA Oncol.* 2019;5:856-863.

18. Gafita A, Weber W, Tauber R, Eiber M. Predictive value of interim PSMA PET during 177Lu-PSMA radioligand therapy for overall survival in patients with advanced prostate cancer. *J Nucl Med.* 2019;60:73.

19. Pollard JH, Raman C, Zakharia Y, et al. Quantitative test-retest measurement of (68)Ga-PSMA-HBED-CC in tumor and normal tissue. *J Nucl Med.* 2020;61:1145-1152.

20. olde Heuvel J, de Wit-van der Veen BJ, Donswijk ML, Slump CH, Stokkel MPM. Day-to-day variability of [68Ga]Ga-PSMA-11 accumulation in primary prostate cancer: effects on tracer uptake and visual interpretation. *EJNMMI Res.* 2020;10:132.

21. Fendler WP, Eiber M, Beheshti M, et al. (68)Ga-PSMA PET/CT: Joint EANM and SNMMI procedure guideline for prostate cancer imaging: version 1.0. *Eur J Nucl Med Mol Imaging.* 2017;44:1014-1024.

22. Gafita A, Bieth M, Krönke M, et al. qPSMA: semiautomatic software for whole-body tumor burden assessment in prostate cancer using (68)Ga-PSMA11 PET/CT. *J Nucl Med.* 2019;60:1277-1283.

23. Pfob CH, Ziegler S, Graner FP, et al. Biodistribution and radiation dosimetry of (68)Ga-PSMA HBED CC-a PSMA specific probe for PET imaging of prostate cancer. *Eur J Nucl Med Mol Imaging.* 2016;43:1962-1970.

24. Feuerecker B, Tauber R, Knorr K, et al. Activity and adverse events of actinium-225-PSMA-617 in advanced metastatic castration-resistant prostate cancer after failure of Lutetium-177-PSMA. *Eur Urol.* 2021;79:343-350.

25. Violet J, Jackson P, Ferdinandus J, et al. Dosimetry of (177)Lu-PSMA-617 in metastatic castration-resistant prostate cancer: correlations between pretherapeutic imaging and whole-body tumor dosimetry with treatment outcomes. *J Nucl Med.* 2019;60:517-523.

26. Gafita A, Calais J, Franz C, et al. Evaluation of SUV normalized by lean body mass (SUL) in (68)Ga-PSMA11 PET/CT: a bi-centric analysis. *EJNMMI Res.* 2019;9:103.

27. Jansen BHE, Kramer GM, Cysouw MCF, et al. Healthy Tissue Uptake of (68)Ga-prostate specific membrane antigen (PSMA), (18)F-DCFPyL, (18)F-Fluoromethylcholine (FCH) and (18)F-Dihydrotestosterone (FDHT). *J Nucl Med.* 2019;60:1111-1117.

Figure 1. Study Flowchart. Abbreviations: PSMA, prostate-specific membrane antigen; mHSPC, metastatic hormone-sensitive prostate cancer; mCRPC, metastatic castration-resistant prostate cancer.

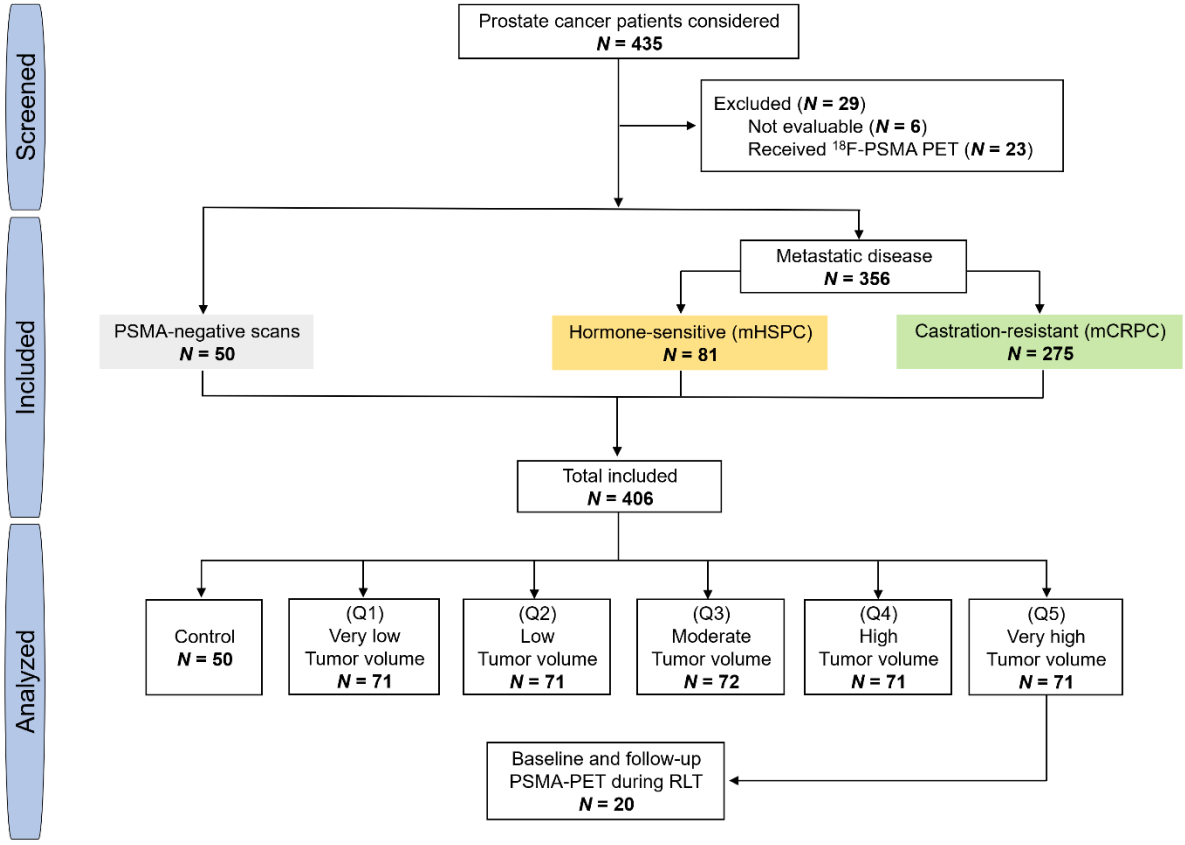

Figure 2. SUV_{mean} of normal organs. Horizontal lines represent the median value.

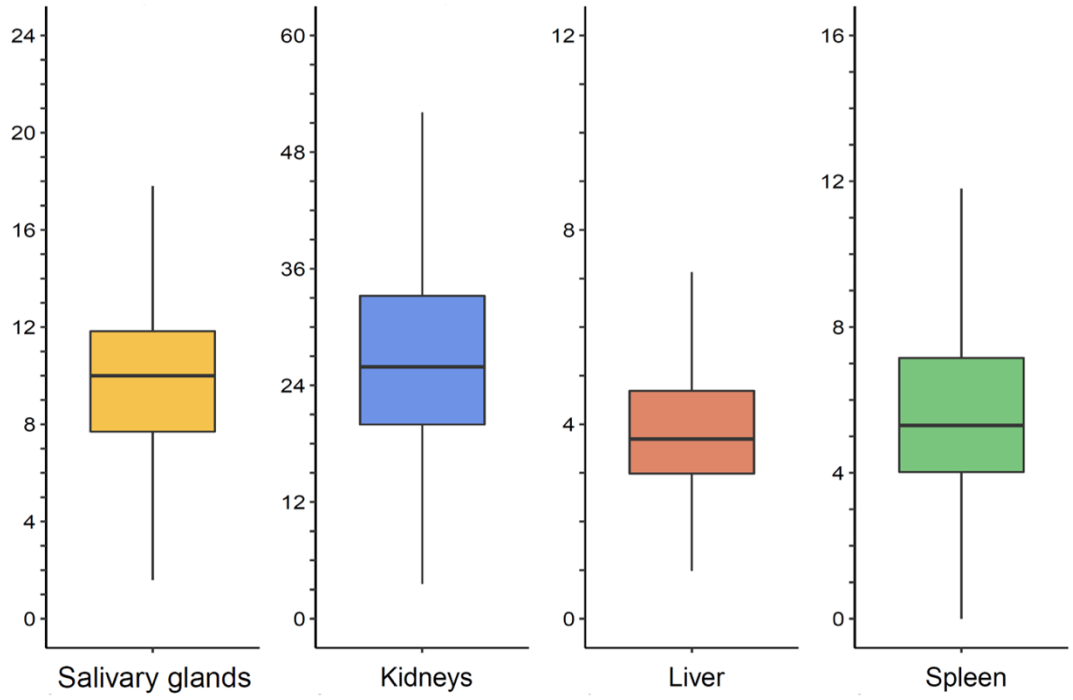

Figure 3. Examples of maximum intensity projection images of PSMA PET for each tumor load group. PSMA-positive tumor segmentation is highlighted in red.

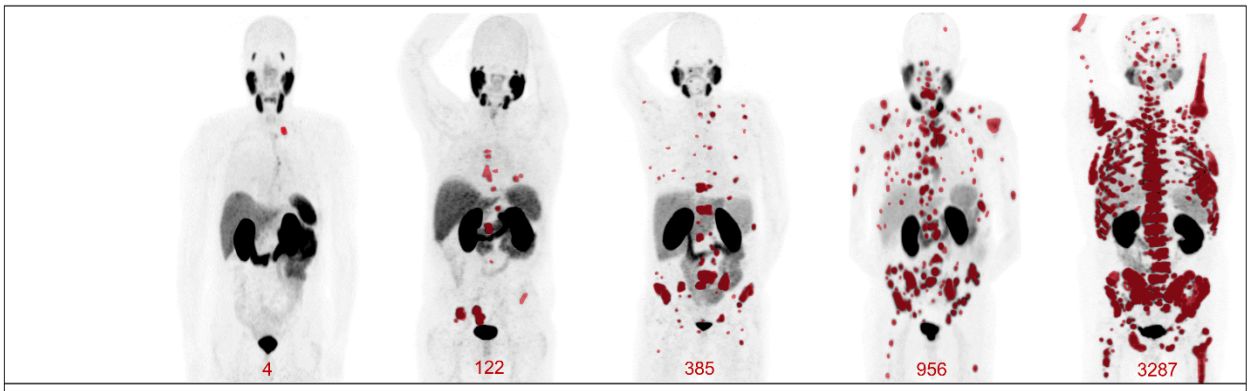

Tumor load:	Very low	Low	Moderate	High	Very high
Quintile:	Q1	Q2	Q3	Q4	Q5
PSMA-VOL (mL):	< 25	25 - 189	189 - 532	532 - 1355	> 1355

Figure 4. SUV_{mean} of normal organs stratified by tumor load.

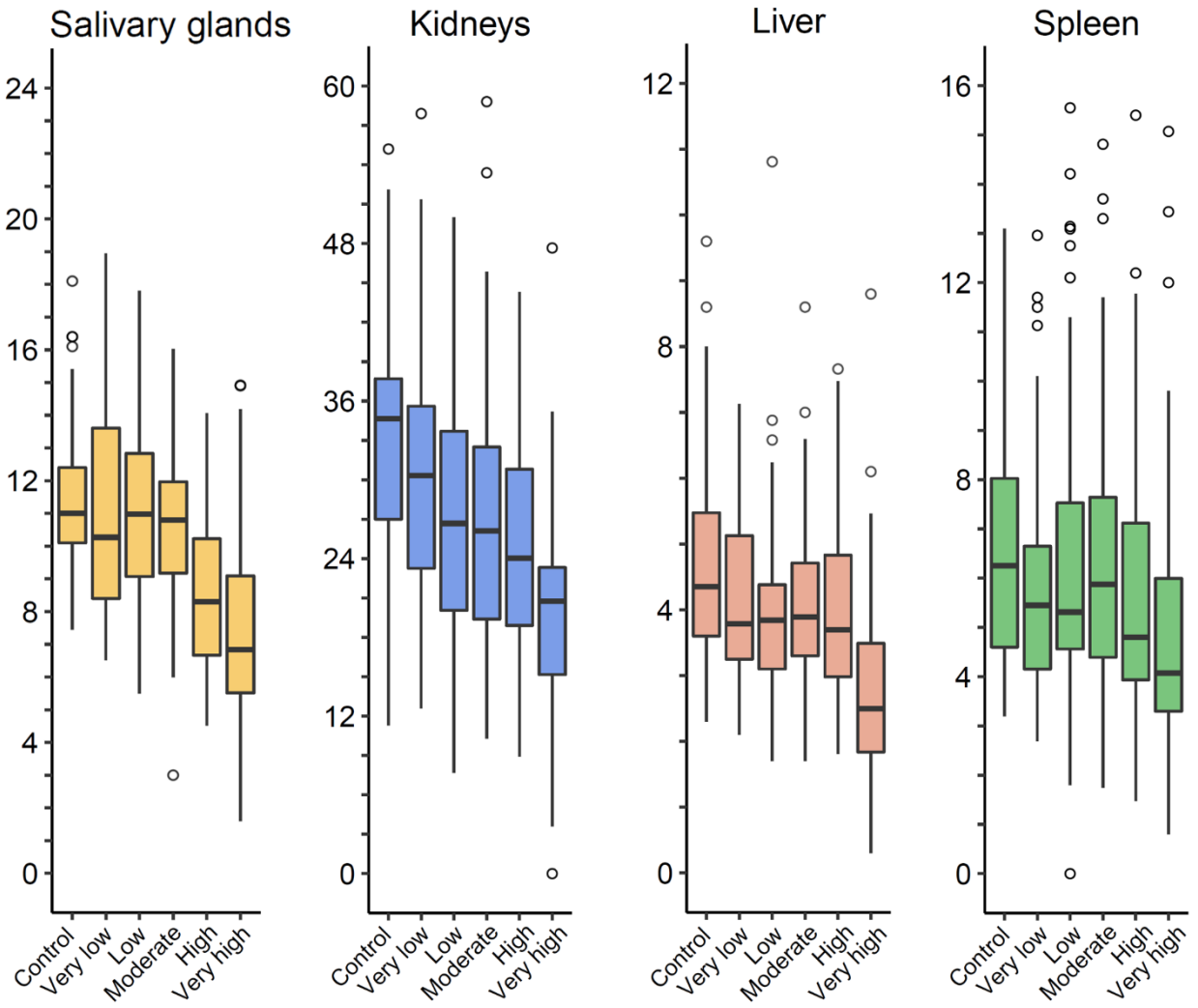

Characteristics	Control (N = 50)	mHSPC (N = 81)	mCRPC (N = 275)
Age (years)	71 (69-74)	69 (63-72)	72 (66-76)
Weight (kg)	86 (80-99)	81 (75-92)	80 (72-92)
Injected Activity (MBq)	185 (183-196)	128 (96-153)	155 (112-195)
Acquisition time (minutes)	60 (55-66)	65 (59-82)	60 (53-67)
PSA (ng/ml)*	0.4 (0.2-0.8)	4.0 (1-11)	130 (37-431)
PSMA-VOL (ml)	0	7 (2-37)	563 (194-1358)
Site of disease on PSMA-PET			
Bone	0	70 (86%)	256 (93%)
Lymph nodes	0	34 (42%)	202 (74%)
Bone + lymph nodes	0	27 (33%)	183 (67%)
Visceral †	0	10 (12%)	82 (30%)
Bone + lymph nodes + visceral	0	1 (1%)	59 (22%)

Table 1. Characteristics of the Patients. Data are median (IQR) or n (%). *Data missing for 10 patients. †Visceral includes lung, liver, rectum, pancreas, peritoneal, brain and adrenal. Abbreviations: PSA, prostate-specific antigen; PSMA, prostate-specific membrane antigen; PSMA-VOL, whole-body PSMA-positive tumor volume; mHSPC, metastatic hormone-sensitive prostate cancer; mCRPC, metastatic castration-resistant prostate cancer.

Table 2. Comparison of PSMA-positive tumor volume groups and [^{68}Ga]^{68}Ga-PSMA-11 uptake in normal organs.

	Tumor Load Group	PSMA-TV	SUVmean			SUVmax		
			Median (IQR)	Differences to Control (95%CI)	*p* value to Control	Median (IQR)	Differences to Control (95%CI)	*p* value to Control
Salivary glands	Control	0 ml	11.0 (10.0 – 12.4)	-	-	21.8 (19.3 – 26.2)	-	-
	Very Low	<25 ml	10.3 (8.3 – 13.7)	-6.4 (-15.2, +3.4) %	0.189	22.9 (18.3 – 29.5)	+5.0 (-4.0, +14.2) %	0.585
	Low	25–189 ml	11.0 (9.1 – 12.9)	+0.5 (-9.8, +10.5) %	0.239	21.9 (18.1 – 29.2)	+0.5 (-9.1, +9.9) %	0.768
	Moderate	189–532 ml	10.8 (9.1 – 12.0)	-1.8 (-9.8, +5.1) %	0.195	23.4 (20.1 – 29.0)	+7.3 (-2.5, +18.0) %	0.352
	High	532–1355 ml	8.3 (6.6 – 10.3)	-24.5 (-33.3, -17.0) %	**<0.001**	18.3 (13.8 – 22.5)	-16.0 (-7.2, -25.5) %	**<0.001**
	Very High	>1355 ml	6.8 (5.5 – 9.4)	-38.1 (-47.8, -29.7) %	**<0.001**	16.0 (11.2 – 23.0)	-26.6 (-15.1, -38.9) %	**<0.001**
Kidneys	Control	0 ml	34.7 (26.4 – 37.8)	-	-	59.8 (49.5 – 68.1)	-	-
	Very Low	<25 ml	30.3 (23.0 – 35.8)	-12.6 (-22.0, +2.2) %	0.125	55.4 (43.8 – 69.5)	-7.4 (-17.8, +3.1) %	0.394
	Low	25–189 ml	26.7 (20.0 – 33.9)	-23.0 (-34.1, -13.5) %	**0.001**	52.6 (37.3 – 69.7)	-12.0 (-22.9, -1.4) %	0.054
	Moderate	189–532 ml	26.5 (19.3 – 32.8)	-23.6 (-32.0, -15.2) %	**<0.001**	54.2 (37.4 – 71.2)	-9.4 (-12.5, +3.0) %	0.085
	High	532–1355 ml	24.0 (18.9 – 31.4)	-30.8 (-42.1, -20.3) %	**<0.001**	47.7 (35.2 – 65.3)	-20.2 (-30.5, -9.8) %	**0.005**
	Very High	>1355 ml	20.8 (15.1 – 23.6)	-40.0 (-50.3, -31.1) %	**<0.001**	42.8 (31.4 – 52.8)	-28.4 (-39.4, -18.0) %	**<0.001**
Liver	Control	0 ml	4.4 (3.6 – 5.5)	-	-	9.5 (8.2 – 11.2)	-	-
	Very Low	<25 ml	3.8 (3.2 – 5.2)	-13.6 (-25.0, +1.6) %	0.070	11.0 (8.5 – 12.4)	15.8 (+2.4, +25.9) %	0.073
	Low	25–189 ml	3.9 (3.1 – 4.5)	-11.4 (-20.3, -3.0) %	**0.010**	10.1 (7.5 – 11.6)	+6.3 (-4.1, +15.2) %	0.886
	Moderate	189–532 ml	3.9 (3.3 – 4.8)	-11.4 (-22.0, -1.7) %	**0.033**	9.9 (8.5 – 12.2)	+4.2 (-9.8, +17.1) %	0.451
	High	532–1355 ml	3.7 (3.0 – 4.9)	-15.9 (-25.9, -16.1) %	**0.008**	9.3 (7.6 – 11.6)	-2.1 (-11.8, +7.9) %	0.842
	Very High	>1355 ml	2.5 (1.8 – 3.5)	-43.2 (-55.6, -30.8) %	**<0.001**	7.8 (6.4 – 10.6)	-17.9 (-30.0, -4.2) %	**0.017**
Spleen	Control	0 ml	6.3 (4.6 – 8.2)	-	-	10.3 (8.2 – 13.4)	-	-
	Very Low	<25 ml	5.5 (4.2 – 6.8)	-12.7 (-25.5, +1.2) %	0.074	10.9 (9.3 – 12.6)	+5.8 (-6.1, +17.6) %	0.384
	Low	25–189 ml	5.3 (4.5 – 7.6)	-14.9 (-30.0, +2.4) %	0.175	10.2 (8.2 – 13.7)	-1.0 (-9.8, +8.0) %	0.888
	Moderate	189–532 ml	5.9 (4.4 – 7.8)	-6.3 (-18.9, +6.2) %	0.422	11.0 (8.4 – 13.9)	+6.8 (-6.2, +19.3) %	0.492
	High	532–1355 ml	4.8 (3.9 – 7.2)	-23.8 (-37.3, -6.8) %	0.012	9.2 (7.5 – 12.9)	-10.7 (-23.9, +3.4) %	0.271
	Very High	>1355 ml	4.1 (3.3 – 6.0)	-34.9 (-49.8, -21.3) %	**<0.001**	9.1 (6.4 – 12.2)	-11.7 (-24.4, +1.9) %	0.068

Supplementary Figure 1. SUV_{max} of normal organs divided by tumor load groups. Horizontal lines represent the median value.

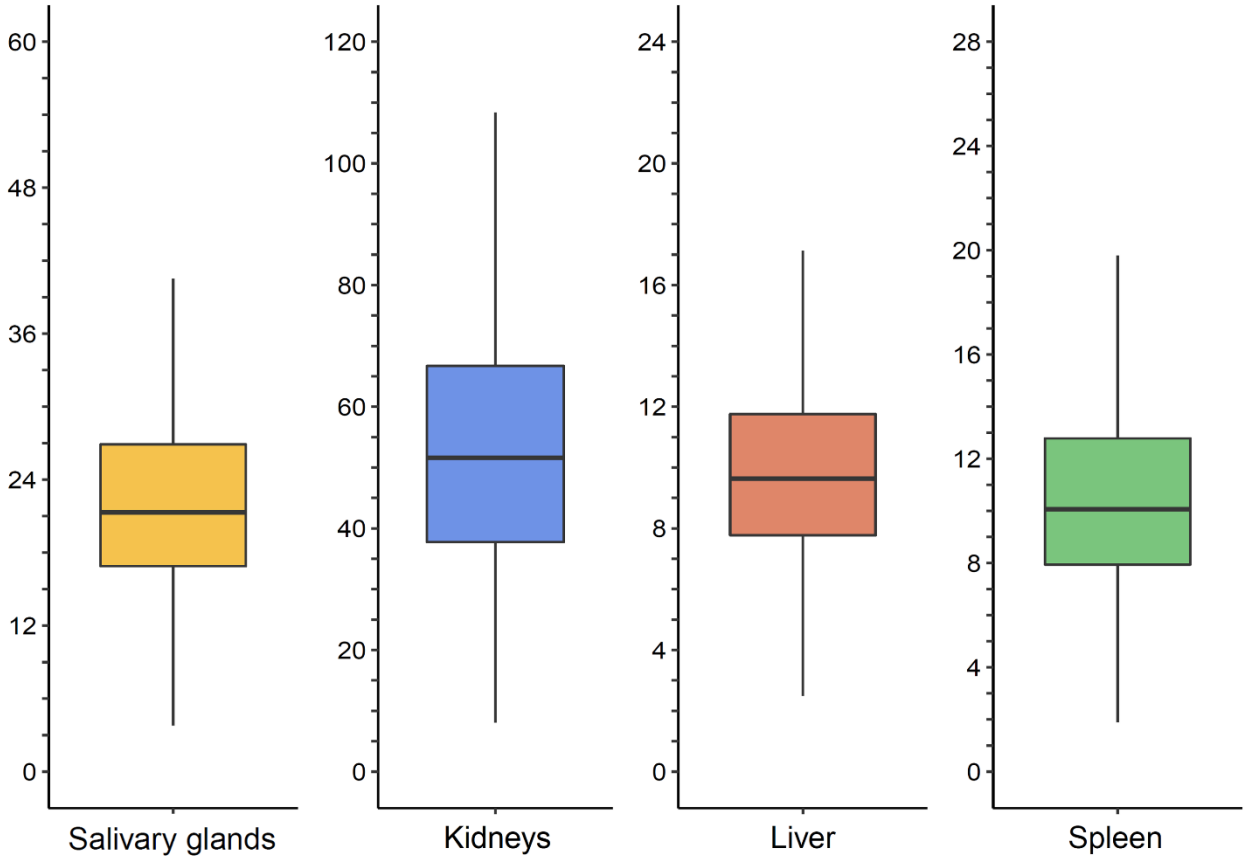

Supplementary Figure 2. SUV_{max} of normal organs stratified by tumor load.

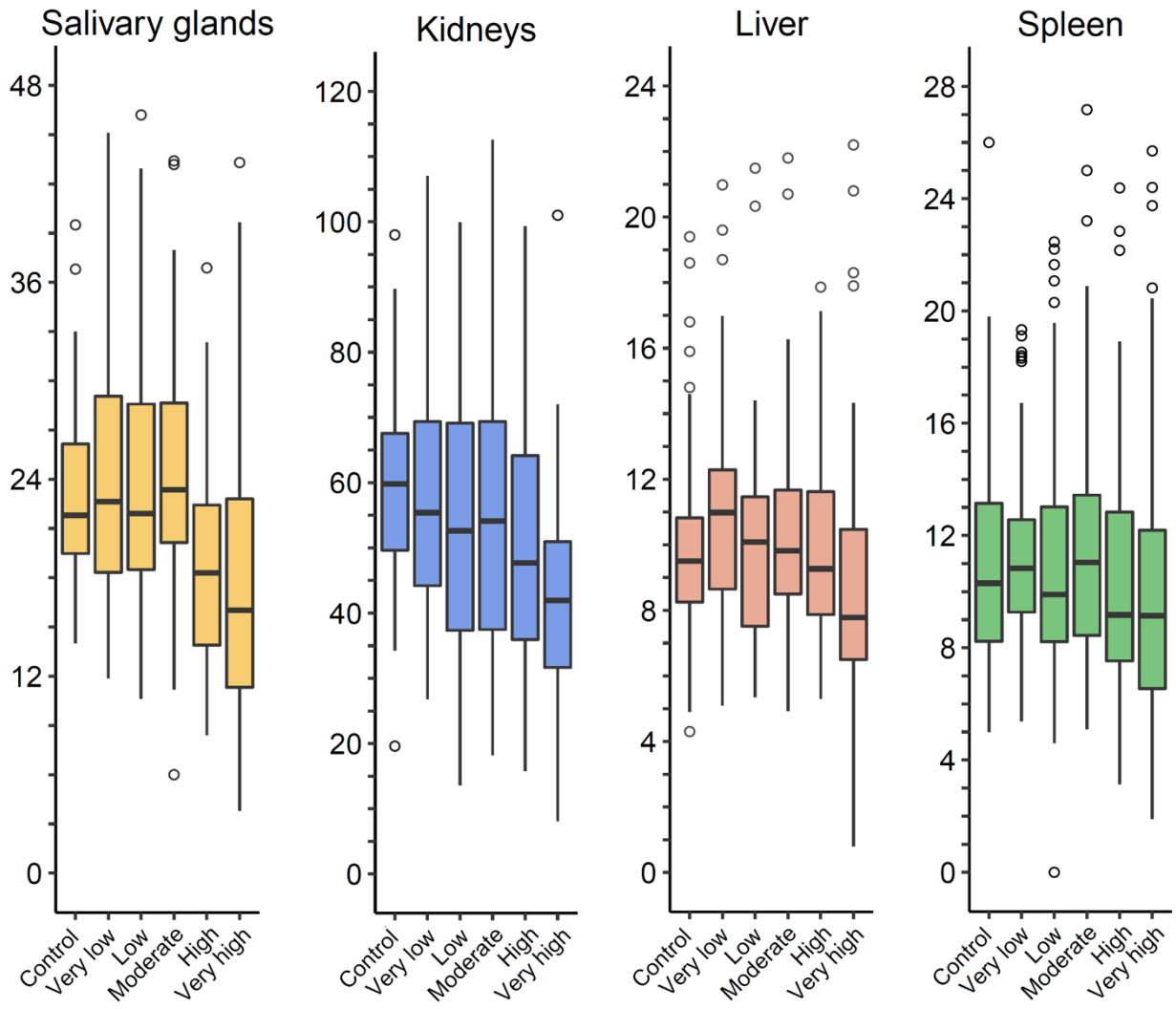

No. Pts.	Center	PET/CT system	Tracer	Matrix Size	Recon-struction algorithm	Point-Spread-Functions	Pixel size (mm)	EANM/SNMMI Guideline
N=124	TUM	Siemens, Biograph mCT	^{68}Ga-PSMA	200x200	PSF-TOF (3i, 21s)	Yes	4.06x4.06	Yes
N=92	UCLA	Siemens, Biograph 64	^{68}Ga-PSMA	200x200	OSEM3D (2i, 24s)	No	4.06x4.06	Yes
N=88	UKE	Siemens, Biograph mCT	^{68}Ga-PSMA	200x200	PSF-TOF (3i, 21s)	Yes	4.06x4.06	Yes
N=50	PMCC	General Electric, Discovery 710	^{68}Ga-PSMA	192x192	VPFXS	Yes	2.9x2.9	Yes
N=32	UKH	Siemens, Biograph mCT	^{68}Ga-PSMA	200x200	PSF-TOF (2i, 21s)	Yes	4.06x4.06	Yes
N=20	EDNOC	Siemens, Biograph 16	^{68}Ga-PSMA	168x168	OSEM3D (2i, 24s)	No	4.06x4.06	Yes

Supplementary Table 1. Overview of the applied reconstruction parameters.

Abbreviations: TUM, Technical University Munich; UKE, University Hospital Essen; PMCC, Peter MacCallum Cancer Center; UKH, University Hospital Heidelberg; EDNOC, Excel Diagnostics Nuclear Oncology Center; PSF, point-spread-function.

				SUVmean								SUVmax							
	PSMA-VOL		NL	Salivary Glands		Kidneys		Liver		Spleen		Salivary Glands		Kidneys		Liver		Spleen	
Subgroup	Bsl	%		Bsl	%	Bsl	%	Bsl	%	Bsl	%	Bsl	%	Bsl	%	Bsl	%	Bsl	%
PSMA-VOL decline ≥30%	2007	-65%	-	11.0	+15%	21.0	+12%	3.5	+103%	6.5	+11%	6.8	+85%	18.5	+455	5.2	+60%	6.1	+49%
	3716	-64%	-	6.9	+112%	13.2	+71%	1.2	+100%	2.8	+118%	32.4	+20%	71.6	+10%	9.6	+35%	12.8	+93%
	2038	-55%	-	14.2	+31%	28.9	+18%	3.2	+58%	4.0	+81%	19.4	-17%	26.7	+0%	8.8	+7%	9.4	+12%
	2136	-55%	-	8.6	+33%	20.7	-16%	2.9	+3%	3.5	+37%	27.6	-12%	57.0	-1%	13.9	+19%	13.0	+1%
	3305	-47%	-	3.8	+84%	10.7	+42%	2.5	+80%	3.5	+65%	35.7	+6%	72.0	+6%	10.7	+16%	12.0	+28%
	2323	-40%	-	7.7	-18%	10.4	+31%	1.8	+22%	4.2	+31%	19.3	-24%	49.2	-23%	-	-	16.0	-27%
	2483	-40%	-	4.4	+14%	19.9	-8%	-	-	8.5	-26%	3.8	+445%	8.1	+195%	1.5	+260%	1.9	+147%
	2004	-39%	-	10.6	+52%	31.2	+3%	3.5	+31%	6.0	+77%	18.3	+26%	43.4	-14%	6.8	+15%	9.3	+8%
	1432	-36%	+	7.8	+4%	35.2	-12%	5.3	+5%	5.4	+52%	14.8	+162%	23.5	+126%	6.3	+65	6.4	+72%
	4251	-31%	-	1.6	+294%	3.6	+219%	0.4	+275%	0.8	+175%	17.4	+5%	66.1	-12%	12.2	-95	11.6	+17%
PSMA-VOL decline <30%	3369	-28%	+	6.8	+7%	15.0	-7%	1.6	-17%	1.5	-22%	21.6	-21%	28.9	+7%	10.5	-62%	9.2	+2%
	2069	-25%	-	10.7	-3%	31.2	+17%	2.7	-4%	4.9	-22%	24.2	-49%	21.3	+23%	3.5	+40%	3.2	+74%
	1549	-18%	+	7.2	-18%	19.0	-3%	3.5	+43%	9.8	-15%	10.2	+34%	40.5	+16%	5.8	+84%	7.5	+33%
	2805	-3%	-	5.1	+19%	23.1	-7%	1.0	+32%	1.6	+39%	18.5	-37%	55.7	-23%	22.2	-48%	24.4	-39%
	2877	4%	+	8.3	-4%	11.2	-7%	2.4	-18%	5.7	+21%	9.5	+9%	46.0	-15%	4.2	+14%	4.0	+16%
	3027	8%	+	5.1	+10%	11.2	+33%	1.2	+23%	1.1	+168%	21.4	-39%	35.1	-15%	7.8	-46%	3.5	-22%
	1891	13%	+	9.2	-44%	21.1	+14%	6.1	-25%	12.0	-29%	11.0	-11%	55.6	+15%	4.8	-6%	3.5	+46%
	3108	14%	+	6.3	-9%	29.7	+16%	2.0	+39%	1.9	+71%	10.9	-1%	24.0	+28%	5.8	-43%	5.7	-7%
	1978	30%	-	5.6	+7%	21.9	+13%	2.6	+27%	3.8	+8%	17.2	-21%	46.0	-19%	20.8	-54%	17.7	-24%
	1964	69%	+	5.5	+9%	13.6	+38%	1.8	+17%	3.0	+19%	23.9	-14%	57.7	+16%	7.7	-6%	9.9	-13%

Supplementary Table 2. PSMA-VOL, SUVmean and SUVmax of normal organs in ^{68}Ga-PSMA-11 PET/CT of 20 patients who received a baseline and follow-up scan during ^{177}Lu-PSMA RLT. Abbreviations: PSMA-VOL, PSMA-avid tumor volume; NL, new lesions; Bsl, baseline; %, percentage change on the follow-up PET scan relative to baseline.